

CFD simulation for hydrodynamic behaviour of fine particles in a fluidized bed

Pranati Sahoo & Abanti Sahoo*

Chemical Engineering Department, National Institute of Technology, Rourkela 769 008, Odisha, India
Email: pranatisahoo02@gmail.com

Received 30 April 2014; accepted 11 August 2015

The fluidization characteristics of fine particles i.e. Geldart–C and A particles are studied in a cylindrical fluidized column. The effects of different system parameters (viz. static bed height, particle density, size of particle, speed of promoter and superficial velocity of the fluidizing medium) on bed dynamics are analyzed. CFD simulation is carried out for the hydrodynamic behaviour of fine powders. The values of these bed dynamics obtained through CFD simulation are compared against the respective experimental values. The comparison results show very good agreement between the experimental and simulated results thereby indicating the possibility of smooth or proper fluidization for fine particles. Thus these findings will be helpful in designing a good fluidized bed reactor for fine particle system can optimize the processes very well.

Keywords: CFD simulation, Eulerian-Eulerian approach, Fine particles, Fluidization, Hydrodynamic studies

Gas–solid fluidized beds are widely used in both the chemical reaction and the physical processes for their excellent gas–solid contacting, maintaining relatively uniform temperature/concentration profiles within the beds and favourable heat and mass transfer characteristics. As the particle size of bed materials decreases the cohesive force for the particle increases. As a result, the fluidization of cohesive materials (i.e. Geldart–C and A particles) becomes more difficult in comparison with the larger sized particles. The fine particles having strong inter-particle forces, small particle sizes and low particle density exhibit problems like plugging, disrupting, agglomerating, bubbling, channeling resulting in poor fluidization of particles. Thus bed tends to rise as a slug of solids¹. The satisfactory performance of any fluidization unit depends upon the quality of fluidization. Therefore it is essential to know the quality of fluidization for which development of a reliable technique to improve the fluidization quality of cohesive fine powders is thought of. This may be achieved by application of external force or by altering the intrinsic properties of particles. Some of the important variables affecting the quality of fluidization are flow rate of fluid, particle size/density of bed materials, static bed height and bed aspect ratio¹. Understanding the hydrodynamics of fluidized bed is essential for their proper design and efficient operations, also for choosing the correct operating parameters for the appropriate fluidization regimes¹⁻³. Gas–solid flows at

high concentrations are quite complex because of the coupling of the turbulent gas flow and fluctuation of particle motions dominated by inter-particle collisions. These complexities lead to considerable difficulties in designing, scaling up and optimizing the operation. The fundamental problem encountered in modeling hydrodynamics of a gas-solid fluidized bed is the motion of two phases where the interface is unknown and transient, and the interaction is understood only for a limited range of conditions^{1,2}. Computational fluid dynamics (CFD) offers a new approach to understand the complex phenomena that occur between the gas phase and the particles in the gas bubbling fluidized beds.

The bed expansion of fine powders has investigated with high aspect ratio⁴. Fine particles are fluidized under reduced pressures where only the upper part of the bed is fluidized and the rest is quiescent for which the minimum fluidization velocity is determined⁵. Experiments on the fluidization of fine particles (0.01–18.1 μm) have been carried out⁶ where particle agglomerates varied in sizes from the largest at the bottom of the bed to the smallest at the top. Uniform fluidization of fine particles ($\leq 50 \mu\text{m}$) have been explained⁷ by the hydraulic resistance of the bed measured as a function of its height and the rotational speed of the mixer during the fluidization process. The effects of vibration/sound amplifier/cross flow magnetic field have investigated on the fluidization of fine particles⁸⁻¹².

Two different CFD models have been applied for modeling gas–solid fluidized bed. They are Eulerian–Lagrangian and Eulerian–Eulerian model. As Eulerian–Eulerian models are more appropriate for fluidized beds¹³, this has also been used in the present work. In this approach, all phases are considered to be continuous and fully interpenetrating. The equations employed are the generalization of the Navier–Stokes equations. The spatially averaged Eulerian–Eulerian equation of motion is first derived¹⁴ where each solid phase is characterized with a size, density and restitution coefficient. One set of the mass and momentum conservation equations are solved for each phase, where the momentum equations are linked by an interphase exchange term. Different averaging methods have been used by various researchers such as time averaging¹⁵ and volume averaging method^{16,17}. Thus, the averaged equations are selected in this work to simulate multiphase flows containing a significant volume fraction of solid particles. On comparing Eulerian–Eulerian and Eulerian–Lagrangian approaches¹⁸ concluded that Eulerian–Eulerian approach is potentially faster than the Eulerian–Lagrangian method, but it requires the formulation of constitutive equations. It is also found that many authors have used the kinetic theory of granular flow to obtain the constitutive equations, in order to describe the rheology of particulate phases.

Experimentally the Eulerian–Eulerian gas–solid simulations of bubbling fluidized bed is verified with the correlations for bubble size or bubble velocity^{19,20}. A computational study for the flow behaviour of a lab scale fluidized bed presented²¹. The results obtained from a ‘discrete particle method’ (DPM) are qualitatively compared with that of a multi–fluid computational fluid dynamic (CFD) model. Two dimensional multi fluid Eulerian CFD model have applied with closure laws according to the kinetic theory of granular flow to study the influence of the coefficient of restitution on the hydrodynamics of dense gas fluidized beds²². Hydrodynamic behaviours of non reactive gas–solid fluidized bed reactor using multi fluid Eulerian model where the effects of particle size and superficial gas velocity are studied^{23,24}. Hydrodynamics of a gas–solid tapered fluidized bed with CFD simulations have reported²⁵.

In normal or smooth fluidization the bed behaviour can be predicted easily. But the bed behaviour is not easily predictable in case of an aggregative fluidization for Geldart–C and A particles. It is also well known that Geldart–C and A particles are

difficult to fluidize under normal conditions due to the action of strong cohesive forces. With a view to improve the quality of fluidization of Geldart–C and Geldart–A (fine) particles a new technique is introduced in the present work. The fluidization process is carried out by using different speed of promoter for applying external force. The objective of the current work is also to develop a CFD model to describe the hydrodynamics of a gas–solid fluidized bed. Kinetic theory of granular flow has been developed to study the hydrodynamic behaviour of fine particles. The effects of gas velocity, particle density and particle size have been investigated experimentally as well as computationally using the CFD. The results of the simulations are finally compared with the experimental findings to check the effectiveness of the model.

Governing Equation

The governing equations of the gas–solid flow include the conservation of mass and momentum. The governing equations of solid and gas phases based on the Eulerian–Eulerian model are as follows.

The volume fractions of the phases sum to one i.e.

$$\varepsilon_g + \varepsilon_s = 1 \quad \dots(1)$$

The continuity equation for gas and solid phases in the absence of inter–phase mass transfer are respectively given as

$$\frac{\partial}{\partial t}(\varepsilon_g \rho_g) + \nabla(\varepsilon_g \rho_g u_g) = 0 \quad \dots(2)$$

$$\frac{\partial}{\partial t}(\varepsilon_s \rho_s) + \nabla(\varepsilon_s \rho_s u_s) = 0 \quad \dots(3)$$

The conservation of momentum for the gas and solid phases are described by

$$\frac{\partial}{\partial t}(\rho_g \varepsilon_g u_g) + \nabla(\rho_g \varepsilon_g u_g u_g) = -\varepsilon_g \nabla p + \nabla \tau_g + \rho_g \varepsilon_g g + F_{i,g} \quad \dots(4)$$

$$\frac{\partial}{\partial t}(\rho_s \varepsilon_s u_s) + \nabla(\rho_s \varepsilon_s u_s u_s) = -\varepsilon_s \nabla p - \nabla p_s + \nabla \tau_s + \rho_s \varepsilon_s g + F_{i,s} \quad \dots(5)$$

The terms τ_g and τ_s are the stress–strain tensors of gas and solid phase respectively. They are expressed as follows.

$$\tau_g = \varepsilon_g \mu_g (\nabla u_g + \nabla u_g^T) + \varepsilon_g \left(\lambda_g - \frac{2}{3} \mu_g \right) \nabla u_g I \quad \dots(6)$$

$$\tau_s = \varepsilon_s \mu_s (\nabla u_s + \nabla u_s^T) + \varepsilon_s \left(\lambda_s - \frac{2}{3} \mu_s \right) \nabla u_s I \quad \dots(7)$$

where the terms $F_{i,g}$ and $F_{i,s}$ of the above momentum equations represent the inter–phase momentum exchange for gas phase and solid phase

respectively. Thus the gas solid inter-phase drag force is expressed as

$$F_{D,gs} = K_{gs}(u_g - u_s) \quad \dots(8)$$

Several drag models for the gas-solid inter-phase exchange coefficient K_{gs} are reported in the literature. The drag model i.e. Gidaspow model is used in the present study which is the combination of Wen and Yu model and the Ergun equation.

The fluid solid exchange coefficient K_{gs} is of the following form

$$\text{When } \varepsilon_g > 0.8, \quad K_{gs} = \frac{3}{4} C_D \frac{\varepsilon_s \varepsilon_g \rho_g |u_g - u_s|}{d_p} \varepsilon_g^{-2.65} \quad \dots (9)$$

When $\varepsilon_g \leq 0.8$

$$K_{gs} = 150 \frac{\varepsilon_s(1-\varepsilon_g)\mu_g}{\varepsilon_g d_p^2} + 1.75 \frac{\rho_g \varepsilon_s |u_g - u_s|}{d_p} \quad (10)$$

where C_D is the drag coefficient proposed by Wen and Yu and is given as

$$C_D = \frac{24}{\varepsilon_g R_{ep}} \left[1 + 0.15(\varepsilon_g R_{ep})^{0.687} \right] \text{ When } R_{ep} \leq 1000 \quad \dots(11)$$

$$C_D = 0.4 \text{ when } R_{ep} \geq 1000 \quad \dots(12)$$

The particle Reynolds number is defined as

$$R_{ep} = \frac{\rho_g d_p |u_g - u_s|}{\mu_g} \quad \dots(13)$$

Constitutive Equations

Constitutive equations are required to close the governing relations and are shown in below.

Solid shear stresses

The solid shear stresses contain shear and bulk viscosities arising from particle momentum exchange due to translation and collision.

$$\mu_s = \mu_{s,col} + \mu_{s,kin} + \mu_{s,fr} \quad \dots(14)$$

where Collision Viscosity,

$$\mu_{s,col} = \frac{4}{5} \varepsilon_s \rho_s d_s g_{o,ss} (1 + e_{ss}) \left(\frac{\Theta_s}{\pi} \right)^{1/2} \varepsilon_s \quad \dots(15)$$

Kinetic Viscosity,

$$\mu_{s,kin} = \frac{\varepsilon_s d_s \rho_s \sqrt{\Theta_s \pi}}{6(3-e_{ss})} \left[1 + \frac{2}{5} (1 + e_{ss})(3e_{ss} - 1) \varepsilon_s g_{o,ss} \right] \quad \dots(16)$$

Frictional Viscosity,

$$\mu_{s,fr} = \frac{p_s \sin \phi}{2\sqrt{I_{2D}}} \quad \dots(17)$$

Bulk Viscosity,

$$\lambda_s = \frac{4}{3} \varepsilon_s \rho_s d_s g_{o,ss} (1 + e_{ss}) \left(\frac{\Theta_s}{\pi} \right)^{1/2} \quad \dots(18)$$

Solid pressure

For granular flow in the compressible regime (i.e. where the solid volume fraction is less than its maximum allowable value), a solid pressure is calculated independently. The solid pressure is composed of a kinetic term and a secondary term due to particle collisions.

$$p_s = \varepsilon_s \rho_s \Theta_s + 2\rho_s (1 + e_{ss}) \varepsilon_s^2 g_{o,ss} \Theta_s \quad \dots(19)$$

Radial distribution function

The radial distribution function g_o is a correction factor that modifies the probability of collision of solid granular phase.

$$\text{For a one solid phase } g_o = \left[1 - \left(\frac{\varepsilon_s}{\varepsilon_{s,max}} \right)^{1/3} \right]^{-1} \quad \dots(20)$$

Granular temperature

The granular temperature for solids phase is proportional to the kinetic energy of random motion of particles. The transport equation derived from kinetic theory takes the following form.

$$\frac{3}{2} \left[\frac{\partial}{\partial t} (\rho_s \varepsilon_s \Theta_s) + \nabla \cdot (\rho_s \varepsilon_s \vec{v}_s \Theta_s) \right] = (-p_s I + \tau_s) : \nabla \cdot \vec{v}_s + \nabla \cdot (K_{\Theta_s} \nabla \cdot \Theta_s) - Y_{\Theta_s} + \Phi_{gs} \quad \dots(21)$$

where the diffusion co-efficient for granular energy, K_{Θ_s} is expressed as follows.

$$K_{\Theta_s} = \frac{15 d_s \rho_s \varepsilon_s \sqrt{\Theta_s \pi}}{4(41-33\eta)} \left[1 + \frac{12}{5} \eta^2 (4\eta - 3) \varepsilon_s g_{o,ss} \right] + \frac{16}{15\pi} (41 - 33\eta) \eta \varepsilon_s g_{o,ss} \quad \dots(22)$$

$$\text{where } \eta = \frac{1}{2} (1 + e_{ss})$$

The collision dissipation of energy,

$$Y_{\Theta_s} = \frac{12(1-e_{ss}^2)g_{o,ss}}{d_s \sqrt{\pi}} \cdot \rho_s \varepsilon_s^2 \Theta_s^{3/2} \quad \dots(23)$$

The transfer of the kinetic energy

$$\Phi_{gs} = -3K_{gs} \Theta_s \quad \dots(24)$$

Experimental Section

Materials

The fluidization characteristics of fine particles are studied in a cylindrical Perspex column of 5 cm ID and 100 cm height. A filter cloth with pores of approx. 40 microns is used as the distributor. This is tightly attached to the bottom of column by placing

in between gasket and flange, so that there is no leakage of air. The calming section is packed with spherical glass beads of size 5 mm for uniform distribution of air to avoid channeling. The column is also covered with filter cloth at the top to prevent the entrainment of the particles. Experimental setup is shown in Fig. 1(a). A stirrer (rod promoter) is used inside the column to provide constant agitation to the bed of fine particles. This rod promoter is hanged from the top of the column and is allowed to rotate by a 5-hp motor as shown in Fig. 1(b). Six numbers of rods each of 6 mm diameter are used in rod promoter. Five numbers of rods having 35 mm length are placed laterally at a spacing of 60 mm between two successive rods. Length of central rod is 350 mm. This Stirrer is hanged from the top of the fluidized column to agitate the bed material.

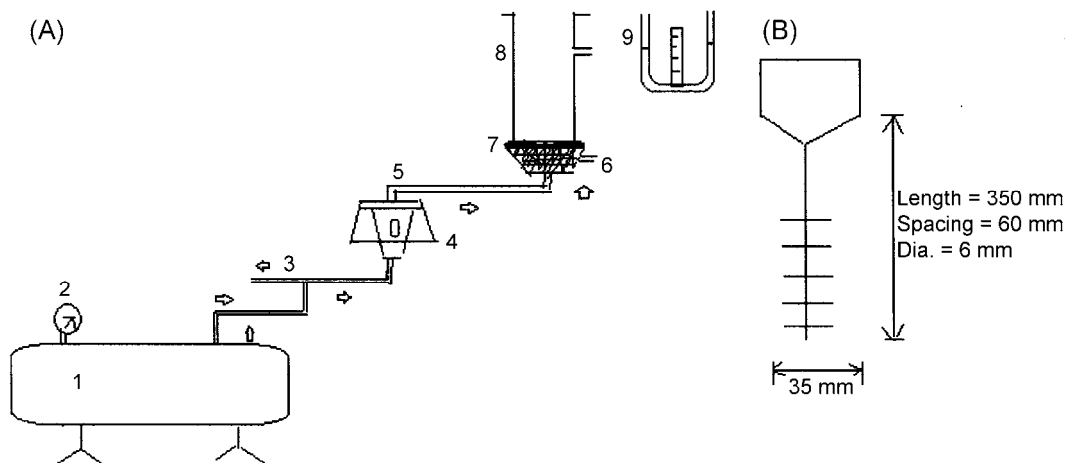
Methods

The bed is loaded with fine particles upto certain height and stirrer is then fitted at the top of the column. Air is supplied from the bottom of the column through a distributor at the ambient conditions. The rotameter and U-tube manometer are connected to the fluidizer for measuring the flow rate of air and the pressure drop across the bed. Carbon tetra chloride (CCl_4) is used as the manometric fluid. Speed of promoter is also made to vary by means of a varriac connected to the motor. The pressure drop and the expanded bed heights (maximum and minimum heights within which the bed fluctuates) are noted against the air flow rates. The scope of the experiment along with the observed bed pressure drop and expansion ratio is shown in Table 1.

Results and Discussion

The CFD software package, FLUENT 13 is used to simulate the gas-solid fluidization process. The CFD simulation is carried out for the fluidized bed of height 1 m and internal diameter 0.05 m for fine particles, where air is considered as working fluid. CFD simulation parameters are shown in Table 2. Standard $k-\epsilon$ dispersed Eulerian granular multiphase model with standard wall functions are used for modeling the transition nature of bubbling fluidized bed. Air is taken as continuous phase while solid particles are taken as dispersed phase which is treated as continua, interpenetrating and interacting with each other and everywhere in the computational domain.

The assumptions like isothermal non-reactive, unsteady state gas-solid system, no lift force, no mass transfer between gas and solid phase, constant pressure gradient and constant density of each phase are considered for CFD simulations. The success of Eulerian-Eulerian approach depends on the proper description of all possible intra and interphase interactions, such as gas-solid interactions, collision and frictional interactions between particles, and interactions between wall and particles. The motion of each phase is governed by its mass and momentum conservation equations. Turbulent fluidization is observed with fine particles in the present work where viscosity is considered to be negligible. Two dimensional (2D) computational geometry has been generated by using commercial software GAMBIT for the fluidized bed. After geometry creation, a uniform mesh i.e. Quadrilateral element structure



1. Compressor; 2. Pressure gage; 3. By pass valve; 4. Rotameter; 5. Control Valve; 6. Calming section with glass bead packing; 7. Distributor; 8. Fluidizer; 9. U tube manometer

Fig. 1—Schematic of experimental unit and stirrer

Table 1 — Scope of the experiment, bed pressure drop and expansion ratio

Materials	Particle density (g/cc)	Particle size (microns)	Static bed height (cm)	Superficial air velocity (m/sec)	Speed of promoter (rpm)	Pressure drop (Pa)	Bed expansion ratio
Alumina powder	0.64	63	16	0.016	121.2	19211.9	1.69
Alumina powder	0.64	63	16	0.021	121.2	20012.4	1.79
Alumina powder	0.64	63	16	0.033	121.2	20679.48	1.84
Alumina powder	0.64	63	16	0.038	121.2	21346.56	1.91
Alumina powder	0.64	63	16	0.046	121.2	21346.56	1.95
Alumina powder	0.64	63	16	0.059	121.2	22680.72	2.01
Alumina powder	0.64	63	16	0.067	121.2	24014.88	2.11
Alumina powder	0.64	63	22	0.021	121.2	22680.72	1.28
Alumina powder	0.64	63	25	0.021	121.2	24948.79	1.35
Alumina powder	0.64	63	28	0.021	121.2	25349.04	1.38
Alumina Powder	0.64	63	16	0.021	73.9	19078.49	1.19
Alumina powder	0.64	63	16	0.021	101.6	20012.4	1.25
Alumina powder	0.64	63	16	0.021	137.4	21613.39	1.3
Silicon carbide	0.72	70	16	0.021	121.2	32686.92	1.89
Talcum powder	0.88	80	16	0.021	121.2	32686.92	2.0
Magnetite	2.4	75	16	0.021	121.2	13940.11	1.39

Table 2 — Parameters used in CFD Simulation

Description	Value	Comment
Particle density	640 kg/m ³	Alumina powder
Particle size	63*10 ⁻⁶ m	Alumina powder
Gas density	1.17 kg / m ³	Air
Gas viscosity	1.8 *10 ⁻⁵ Pa s	Air
Superficial gas velocity	0.016 to 0.067 m/s	≈ 0.4 -1.6 U _{mf}
Bed height	1 m	Fixed value
Bed width	0.05 m	Fixed value
Initial static bed height	0.16 m	Fixed value
Static bed voidage	0.9	Fixed value
Grid interval spacing	0.002 m	Specified
Time steps	0.001 s	Specified
Inlet boundary conditions	Velocity	Superficial gas velocity
Outlet boundary conditions	Outflow	Fully developed flow
Maximum number of iterations	30	Specified
Convergence criteria	10 ⁻³	Specified
Restitution coefficient	0.9	Specified

(height to width ratio of 1) is also generated. In this study, total of 12500 numbers cells with cell size of 0.002m × 0.002m are used for simulating fluidized bed.

Initially solid particle velocity is set at zero (i.e. in minimum fluidization) and the inlet gas velocity at the bottom of fluidized bed is assumed to be uniform along the axial direction. The pressure is not specified at the inlet because of the incompressible gas phase

assumption (relatively low pressure drop system). Pressure boundary condition is specified at the outlet only where no-slip boundary condition is assumed.

The phase coupled SIMPLE method²⁶ is chosen for pressure-velocity coupling and first order upwind scheme is used for discretization of volume fraction equation whereas second order upwind scheme is used for discretization of momentum, turbulent kinetic energy and turbulent dissipation rate. In the discretization process, the governing partial differential equations are converted to algebraic equations. The time step is chosen as 0.001 of 1000 steps. The convergence criteria for all the numerical simulations are based on monitoring of the mass flow residual. The residual value is found to be converging around 1.0e⁻⁰³. The simulation is carried out using different flow quantities till the system reaches quasi-steady state.

Contours of solid volume fraction

The hydrodynamic behaviours of fluidized bed are analyzed by monitoring the contour plots for volume fraction of bed materials, static pressure of bed, velocity magnitude of fluid etc. The bed dynamics of fluidized bed are analyzed by monitoring the phase volume fractions as shown in Figs 2 and 3 in turbulent condition. From Fig. 2, it is observed that bed profile/bed height increased up to 25 sec after which it remained constant upto 60 sec. The fully developed Quasi-steady state is reached after 30 sec where

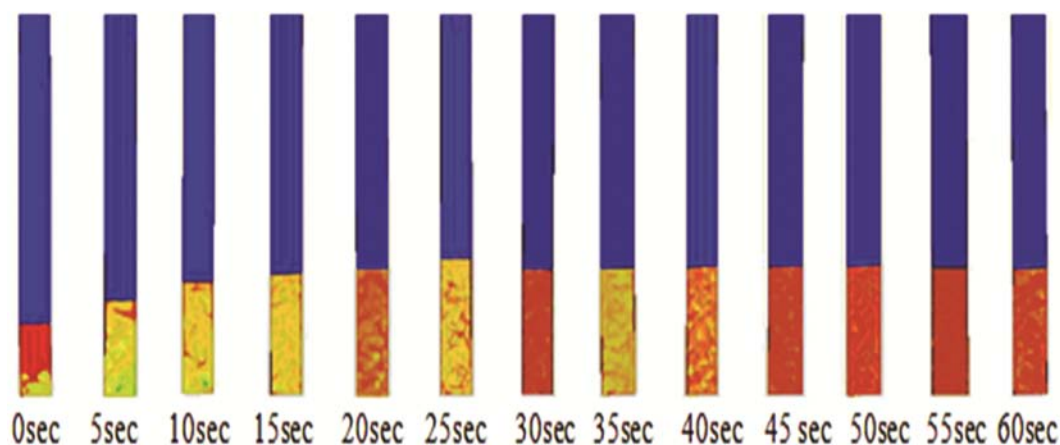


Fig. 2—Contour plot of volume fraction of alumina powder with respect to time

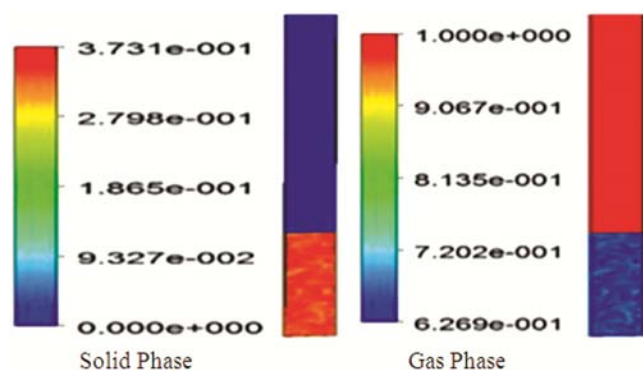


Fig. 3—Contour plot of volume fraction of solid and gas phase for alumina powder

average value of dynamic flow characteristics is calculated in terms of time in both axial and radial direction. The phase dynamics of solid and gas phase is represented in the form of contour plot as shown in Fig. 3. The contour plot of solid phase illustrates that bed is in fluidized condition. The contour plot of gas phase illustrates more gas hold up than the fluidized solid (i.e. volume fraction of solid is less compared to gas) in two phase region.

Phase velocity

The magnitude of velocity vectors for solid phase and gas phase are obtained only after the quasi steady state achieved. The XY plot (Fig. 4), shows the velocity magnitude of gas phase in radial direction. It is seen that air velocity follows parabolic path. It is also found that a peak value for air velocity / maximum outlet velocity of air is 0.023 m/s. Velocity of air is found to be zero at the wall of the fluidization column.

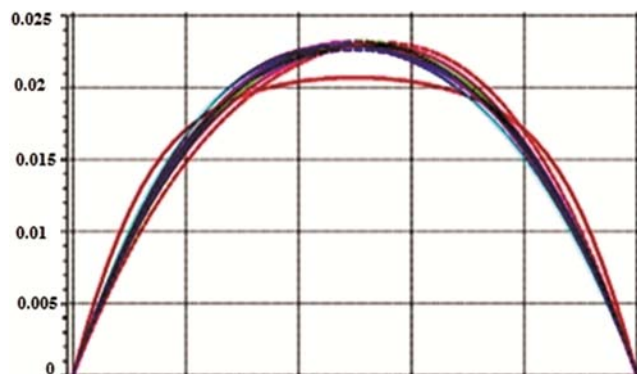


Fig. 4—XY Plot of velocity magnitude in gas

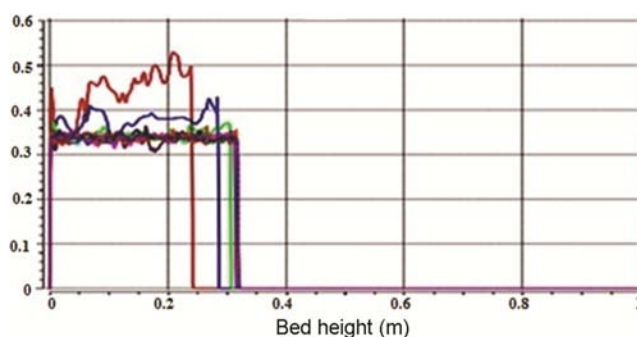


Fig. 5—XY Plot of solid volume fraction

The bed height can also be calculated from XY plot of solid volume fraction (Fig. 5). It is observed that solid volume fraction increases in axial direction with minimum value at bottom of the column. A point is reached where the solid volume fraction sharply decreases to zero indicating the condition of the maximum fluidization. From this figure maximum expanded bed height is obtained as 37 cm.

Contour of superficial velocity of air as shown in Fig. 6(a). It is observed that the superficial velocity of air decreases from 0.061 m/s to 0.017 m/s from bottom to top of the bed which implies that bed materials obstruct the movement of air thereby decreasing the magnitude of air velocity. Finally the air moves upward through the freeboard of the column after achieving minimum fluidization condition.

The velocity vectors for alumina powder and air achieved after the quasi steady state are shown in Fig. 6(b). From velocity vector of solid phase, it is observed that there is vigorous movement of solid particles throughout the bed indicating that the velocity at the bottom is small. It is also observed that in the upper part of bed i.e. in fluidizing section, circulatory motion (i.e. downward motion of the solid particles near the wall region and upward motion in central region of the column) is observed.

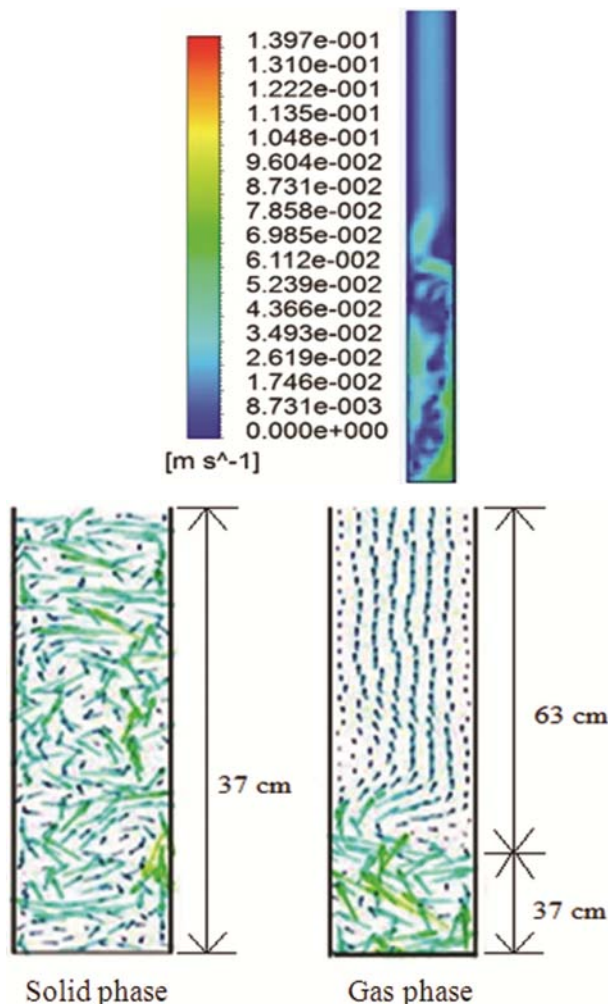


Fig. 6 (a)—Contours of velocity magnitude; (b)—Velocity vector of different phases for fine particles

In case of gas phase, air flow is always observed in upward direction throughout the column (Fig. 6(b)). In the upper section of the column air velocity are high because carrying air bubbles along with it. But in the lower section of the column solid particles obstruct the movement of bubbles so air velocity reduces. When gas moves from main bed region to freeboard region, the air velocity significantly changes. The transition from low to high velocity for flow of air is clearly observed in this figure.

Bed pressure drop

Contours of static pressure of bed materials are shown in Fig. 7(a). It is observed that static pressure decreases from 6.6×10^2 Pa to 1.73×10^2 Pa. Initially bed pressure drop increases with velocity of flow. Once the bed unlocks the bed pressure drop decreases to some extent and then remains constant when bed is perfectly fluidizes. The static pressure of bed material decreases from bottom to top of bed indicating that the top layer of bed material fluidizes first, causing the static pressure to decrease in comparison with the packed bottom portion of bed. Variation of pressure drop with superficial air velocity is shown in Fig. 7(b). It is seen

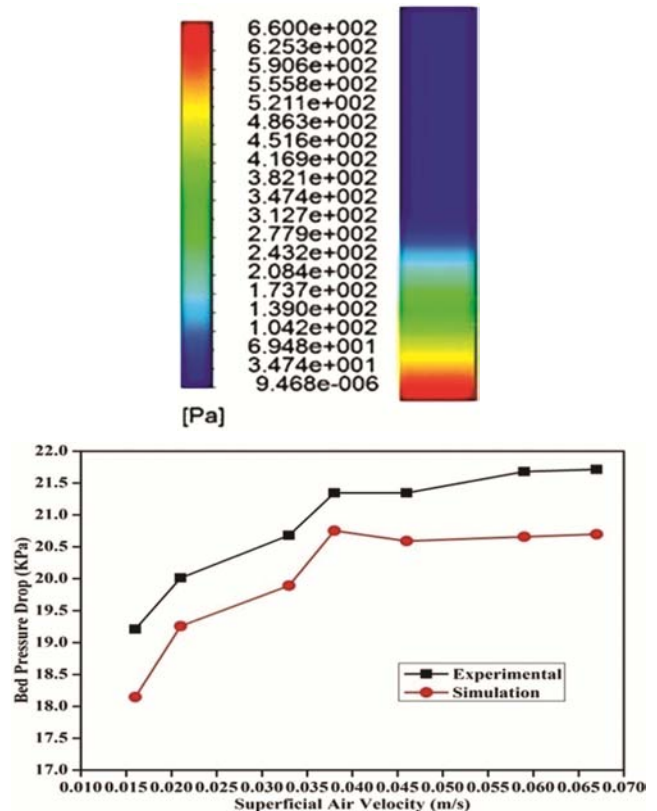


Fig. 7 (a)—Contours of static pressure of bed materials; (b)—Variation of pressure drop with superficial air velocity for fine particles

that the bed pressure drop increases initially upto certain limit then remain constant once minimum fluidization is attained. Similar trends are also observed in simulation case of fine particles fluidization process. From Fig. 7(b), it is also found that simulated results are in good agreement with experimental results with a deviation of 4.11% approximately.

Influence of bed height

Contour plots of bed height for fine particles are shown in Fig. 8(a). It is seen that bed expansion gradually increases with time. Bed height is measured against superficial air velocity both experimentally as well as computationally. Finally experimental and simulation results are compared with each other (Fig. 8(b)). The bed height increases with velocity of fluid indicating that the bed expands more with increase in superficial velocity of fluid. It is observed that simulated results are in good agreement with experimental results with a deviation of - 8.38% approximately.

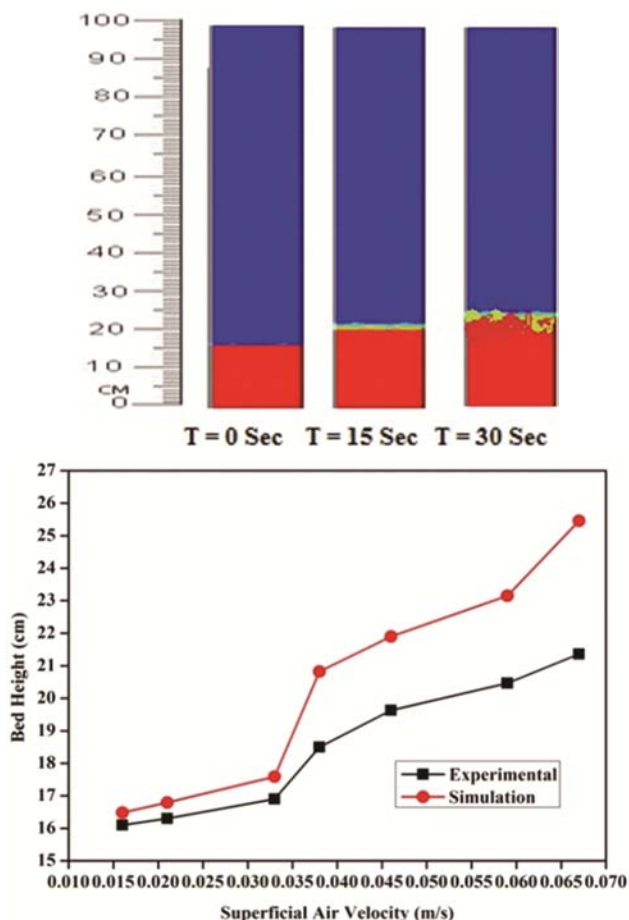


Fig. 8 (a)—Contours of bed height; (b)—Variation of bed height with superficial velocity for fine particles

Effects of inlet velocities

It is observed that the expanded bed height for gas–solid system increases with increase in air velocity indicating that the bed voidage / air volume fraction increases. Experimentally the similar trend is also observed. The bed height of the column is calculated in terms of volume fraction of air. It is found that simulated results are in good agreement with experimental results with a deviation of 2.75% approximately.

The influence of particle size / density

Experimentally, the expanded bed height is also calculated by varying particle density and particle size for solid particles. A comparison is made with CFD simulation. It shows that with increase in particle size and density, the solid volume fraction decreases i.e. expanded bed height decreases. It is understood that simulated results are in good agreement with experimental results with 5.38% deviation (approx.). It is also observed that bed expansion ratio increases with density upto certain level and then decreases. The reasons for this may be the bubbles initially cause the fluidization thereby increasing bed expansion ratio. But as density of particle increases terminal velocity increases which causes the downward movement of particles faster which in turn break the bubbles or obstruct the bubble movement further which results in decrease of bed expansion which is seen with Magnetite material.

Conclusion

Bed hydrodynamics for fine particles are studied both experimentally and computationally using a commercial CFD software package, FLUENT 13. The simulated values of the bed dynamics are observed to be agreeing well with the respective experimental values of bed dynamics at the ambient conditions. Very good agreement of the CFD simulated values with the experimental values indicates that Eulerian-Eulerian multi-phase granular flow approach is capable of predicting the overall performance of gas-solid fluidized bed. The bed dynamics in turbulent fluidized bed for 63 micron sized alumina particles increases with superficial air velocities and time respectively. The magnitude and behaviour of velocity vectors for alumina powder are also calculated after the quasi steady state is achieved in the turbulent fluidized column. The experimental and CFD simulated results are compared with respect to bed expansion ratio and pressure drop. Thus the

bed dynamics of gas–solid fluidization system in turbulent condition are obtained from CFD simulation which is validated thereby against experimental results.

Fluidized bed as well as the spouted bed can be well designed with the knowledge of these bed dynamics. Knowledge of CFD simulations for fluidization system which gives ideas by the visual observations of bed dynamics thus will be very much useful in designing any fluidization process. The knowledge of these bed dynamics obtained computationally and experimentally thus gives the fundamentals for optimum design of gasifiers, combustors, granulators and fluidized bed reactors, especially for the pharmaceutical industries with the provision of employing some external force. Such design can also be extended to nano scale where external force has to be applied to break the cohesive forces among the particles.

Acknowledgements

This work was supported by funding from the National Institute of Technology, Rourkela. The authors thank Dr. (Mrs.) Abanti Sahoo of National Institute of Technology, Rourkela, for her support.

Nomenclature

d	Diameter
ϵ	Volume fraction
ρ	Density of fluid
u	Velocity
p	Pressure
τ	Stress-strain tensor
g	Acceleration due to gravity
F	Force
μ	Viscosity
K_{gs}	The fluid-solid and solid-solid exchange coefficient
I_{2D}	Second invariant of the deviatoric stress tensor
Re	Reynolds number
e_{ss}	Coefficient of restitution
$g_{0,ss}$	Radial distribution co-efficient
C_D	Drag co-efficient
$C_{fr,gs}$	Coefficient of friction of solid phase particles
θ_s	Solid phase granular temperature
μ_s	Solid shear viscosity
$\mu_{s,col}$	Collision viscosity
$\mu_{s,kin}$	Kinetic viscosity
$\mu_{s,fr}$	Frictional viscosity
λ_s	Bulk viscosity
ϕ	Angle of internal friction
K_{θ_s}	Diffusion co-efficient
Υ_{θ_s}	Collisional dissipation of energy
Φ_{gs}	Energy exchange of solid phase
	Rate exponent

\vec{v}_s	Phase-weighted velocity
∇	Gradient

Subscripts

g	Gas
t	Turbulent
s	Solids

Abbreviation

CFD	Computational Fluid Dynamics
2-D	Two Dimensional
GFM	Granular Flow Model
GAMBIT	Geometry and Mesh Building Intelligent Toolkit
SIMPLE	Semi-implicit Method for Pressure-linked Equations
DPM	Discrete Particle Method

References

- Kunii D & Levenspiel O, *Fluidization Engineering*, 2nd Edn, (Butterworth-Heinemann, Boston, Mass, USA) 1991.
- Gidaspow D, *Multiphase Flow and Fluidization*, 1st Edn, (Academic Press, London, UK) 1994.
- Ranade V V, *Computational Flow Modeling for Chemical Reactor Engineering*, 1st Edn (Academic Press, New York, USA) 2002.
- Avidan A A & Yerushalmi J, *Powd Tech*, 32 (1982) 223.
- Kusakabe K, Kuriyama T & Morooka S, *Powd Tech*, 58 (1989) 125.
- Wang Z, Kwauk M & Li H, *Chem Eng Sci*, 53 (3) (1998) 377.
- Laszuk A, Pabisand M & Berengarten G, *Chem & Petro Eng*, 44 (9) (2008) 6.
- Jaraiz E, Kimura S & Levenspiel O, *Powd Tech*, 72 (1992) 23.
- Russo P, Chirone R, Massimilla L & Russo S, *Powd Tech*, 82 (1995) 219.
- Mawatari Y, Tsunekawa M, Tatemoto Y & Noda K, *Powd Tech*, 154 (2005) 54.
- Xu C & Zhu J, *Powd Tech*, 161 (2006) 135.
- Valverde J M, Espin M J, Quintanilla M A S & Castellanos A, *Phy Rev*, 79 (2009) 031306.
- Pain C C, Mansoorzadeh S & Oliveira C R E, *Int J Multiphase Flow*, 27 (2001) 527.
- Anderson T B & Jackson R, *Ind & Eng Chem Fund*, 6 (4) (1967) 527.
- Drew D A & Lahey R T, *Int J Multi phase Flow*, 5 (4) (1979) 243.
- Harlow F H & Amsden A A, *J Comp Phy*, 17 (1975) 19.
- Ahmadi G, *Adv Water Res*, 10 (1987) 32.
- Gera D, Gautam M, Tsuji Y, Kawaguchi T & Tanaka T, *Powd Tech*, 98 (1998) 38.
- Wachem^a B G M V, Schouten J C, Bleek C M V, Krishna R & Sinclair J L, *AIChE J*, 47 (2001) 1035.
- Wachem^b B G M V, Schouten J C, Bleek C M V, Krishna R & Sinclair J L, *AIChE J*, 47 (2001) 1292.
- Chiesa M, Mathiesen V, Melheim J A & Halvorsen B, *Comp & Chem Eng*, 29 (2005) 291.
- Goldschmidt M J V, Kuipers J A M & Swaaij W P M, *Chem Eng Sci*, 56 (2001) 571.
- Taghipour F, Ellis N & Wong C, *Chem Eng Sci*, 60 (2005) 6857.
- Hamzehei M, Rahimzadeh H & Ahmadi G, *J Mech*, 26 (3) (2010) 267.
- Sau D C & Biswal K C, *App Math Mod*, 35 (2011) 2265.
- Patankar S V, *Numerical heat transfer and fluid flow*, 1st Edn (Hemisphere, Washington) 1980.